A Low-Complexity Algorithm for Robust Intrusion Detection in PIR-based Wireless Sensor Network

Ramanathan Subramanian
sramanathan@csa.iisc.ernet.in

Under the guidance of Prof. P. Vijay Kumar

CSA Dept.
IISc, Bangalore

May 17, 2010



Outline

- Problem Description.
- PIR Sensor Operation.
- Intrusion Detection Algorithm Description.
- Simulation Results and Field Testing.
- Idealized Intruder Waveform Analysis.
- Intruder Tracking.



Introduction

- Wireless sensor networks find numerous applications. To name a few,
  - Unattended Surveillance.
  - Environmental applications.
  - Precision Agriculture.
- Surveillance cameras are expensive and power hungry.
- Power outlets are not going to be available in the terrains of interest.
- Currently, Passive Infra-Red (PIR) sensors consume less power than cameras by up to two orders of magnitude.
- PIR sensors can be used as a low-power wake-up mechanism for cameras.
- PIR sensors are triggered by blowing debris, birds, animals, vegetation, hot air currents etc.
- The problem is challenging because intrusion is a rare event while clutter is always present.
- Frequent false alarms would effectively render the system useless.



Problem Description

- Detect an **intruder** in the presence of **clutter** with low false alarm rate.
- The intruder is a human traveling in the vicinity of the sensor.
- The term clutter is used to describe the waveform generated at the output of the sensor as a result of the movement of vegetation caused by the wind.



Objective

- Robust intruder detection algorithm.
- Minimize the energy spent in detection.



Challenges

- Handle various speeds of the intruder.
  - Duration of the intruder signature could vary from $3s$ to $18s$.
- Reject clutter from various forms of vegetation.
  - Performance of the algorithm should not be terrain dependent.
- Low-complexity algorithm.
  - Energy spent in the detection reflects in the number of operations performed.



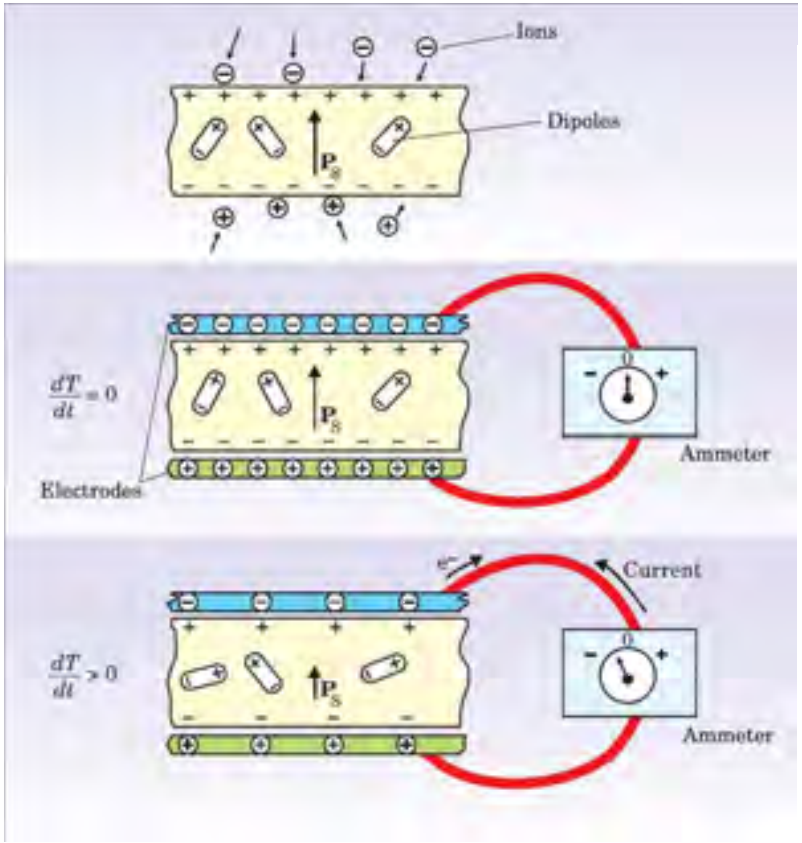
PIR Sensor Operation

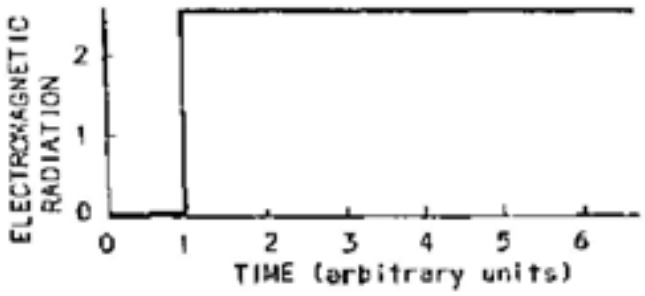
- The PIR sensors along with the optical filters are tuned to detect wavelengths in the range of $8 - 14\mu m$.
- From Wien's law we know that humans emit peak radiation at $9.4\mu m$ (far Infra-Red).
- A PIR sensor converts the spatial and temporal variations of intensity of IR falling onto its sensitive element(s), into an electrical signal.
- Moving vegetation also causes variations in the ambient IR intensity perceived by the sensor, which leads to clutter. This is primarily due to varying occlusions of background IR emissions caused by moving vegetation.

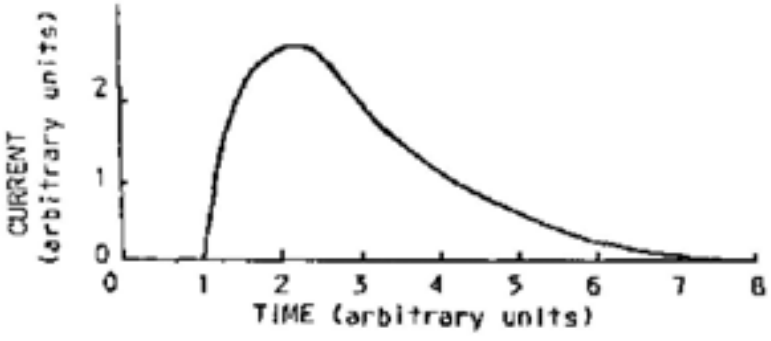


Pyroelectricity

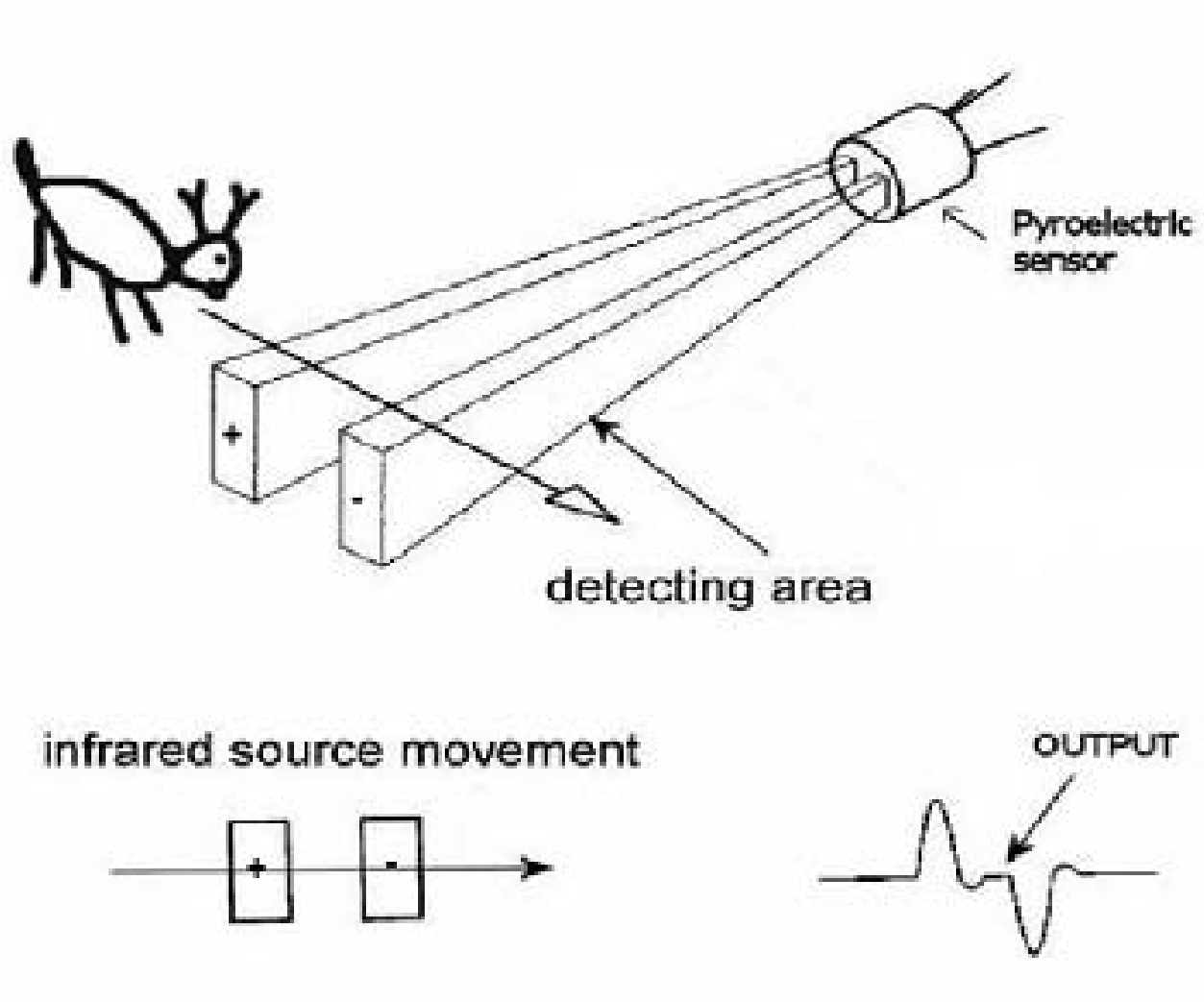
- A PIR sensor works on the principle of pyroelectricity.





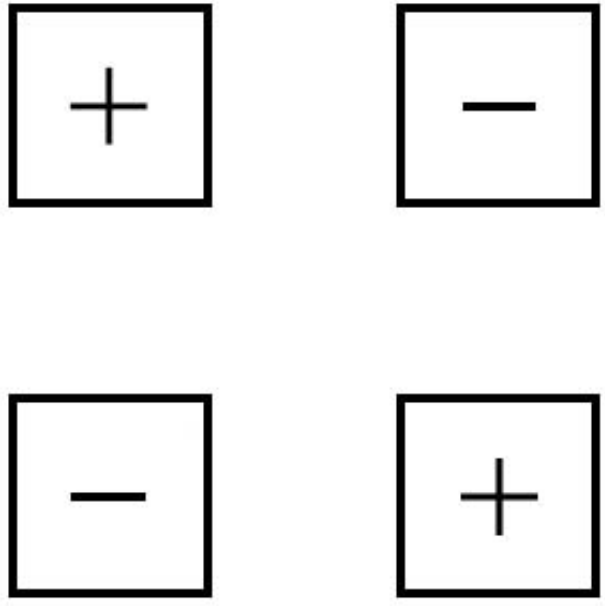


Basic Sensing Model



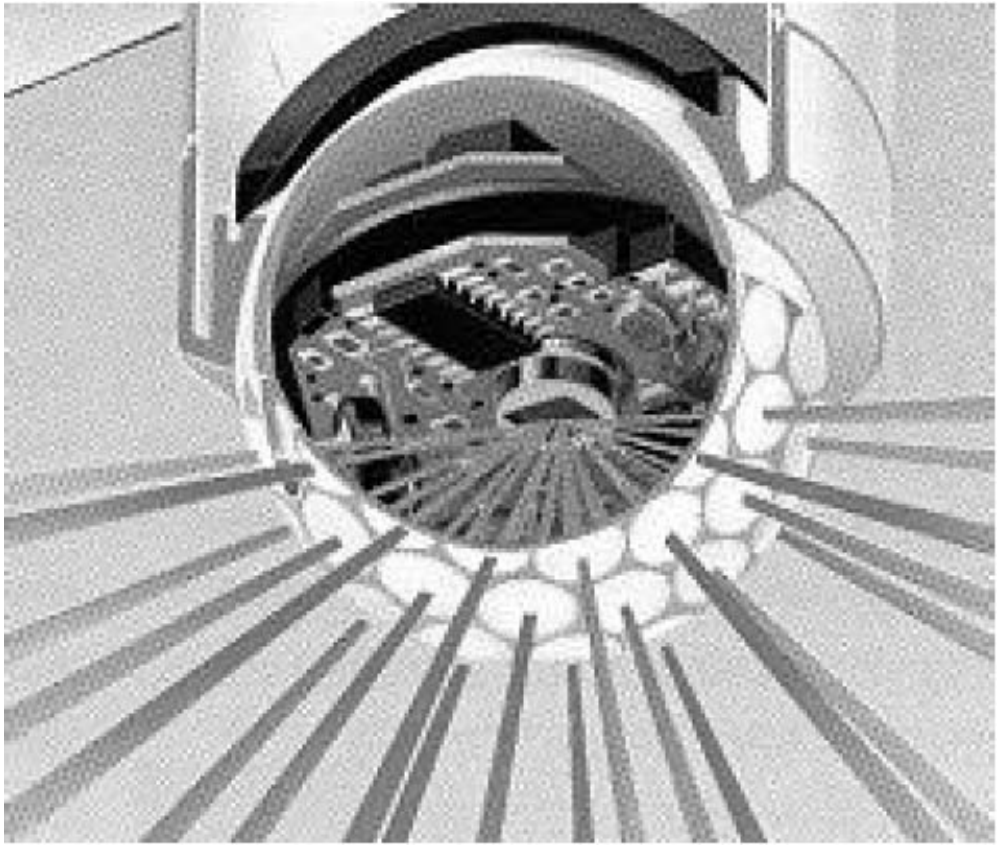
Analog Panasonic Motion Sensor *AMN*24111





- The sensor produces an electrical potential proportional to differences in the rate of intensity variations across the two diagonals.

Golf Ball Lens



- Radiation received by each plano-convex lens from a zone in the field of view is focused in the sensing region for sensing by the infrared detector.

Cross Section Of The Beams

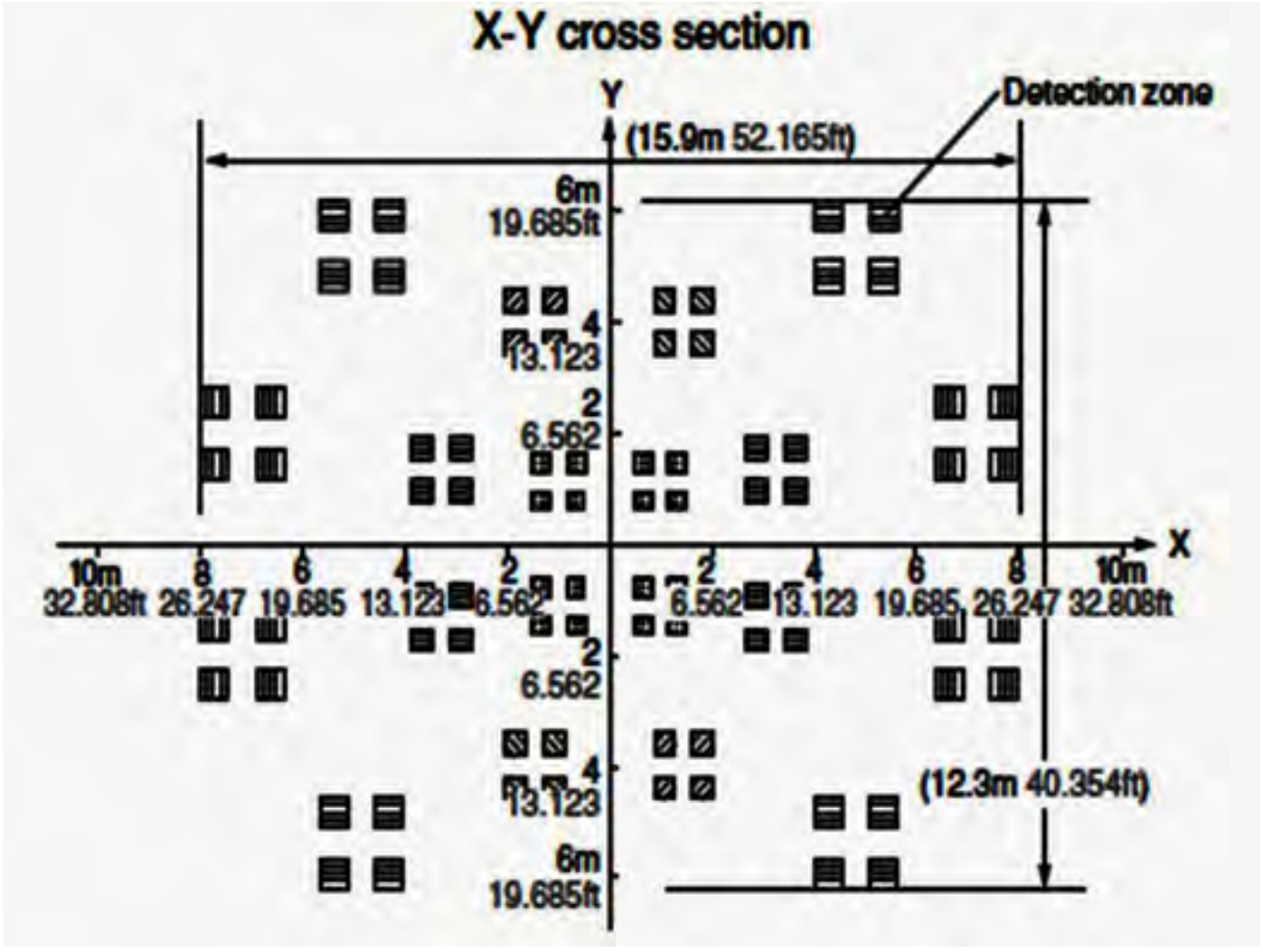
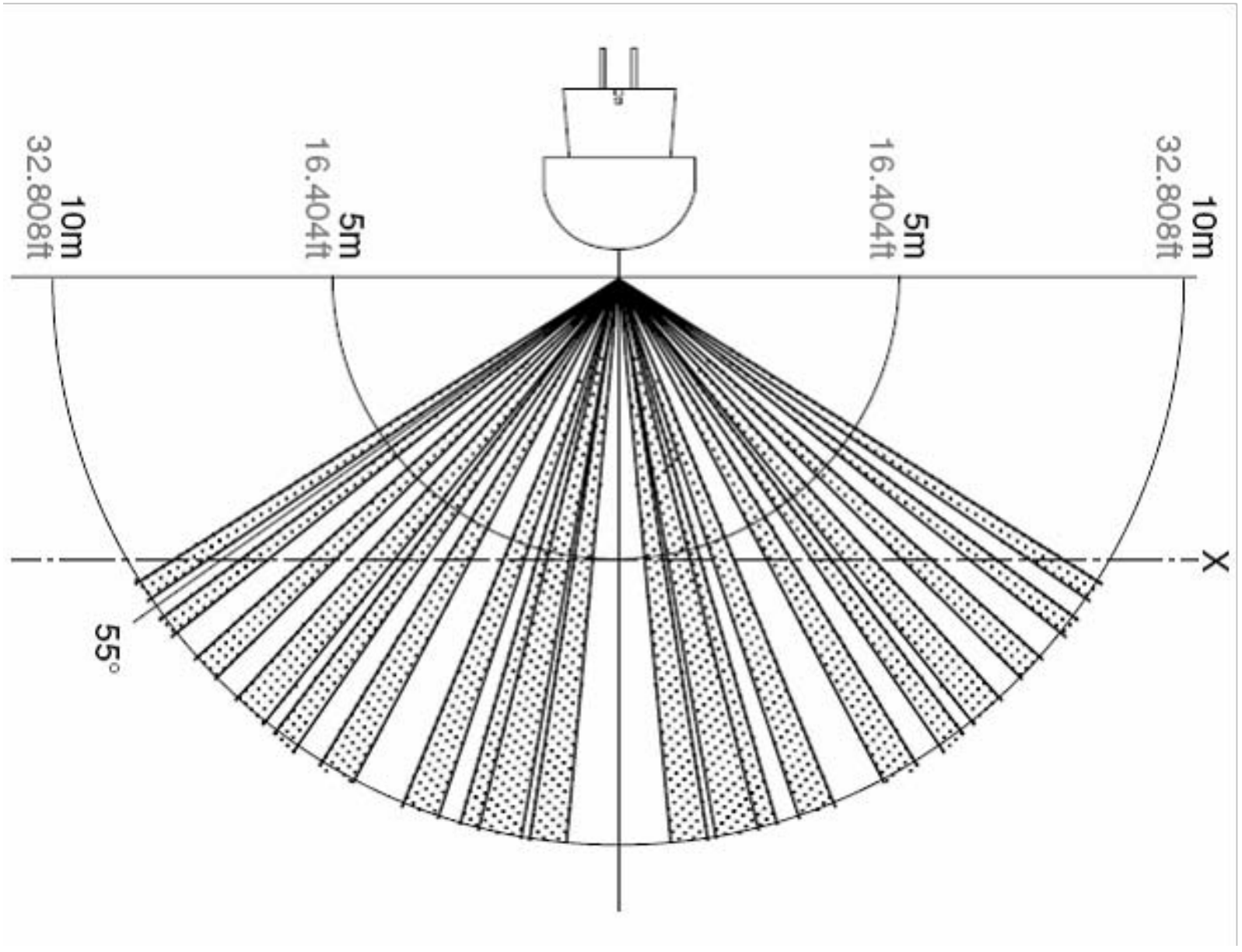
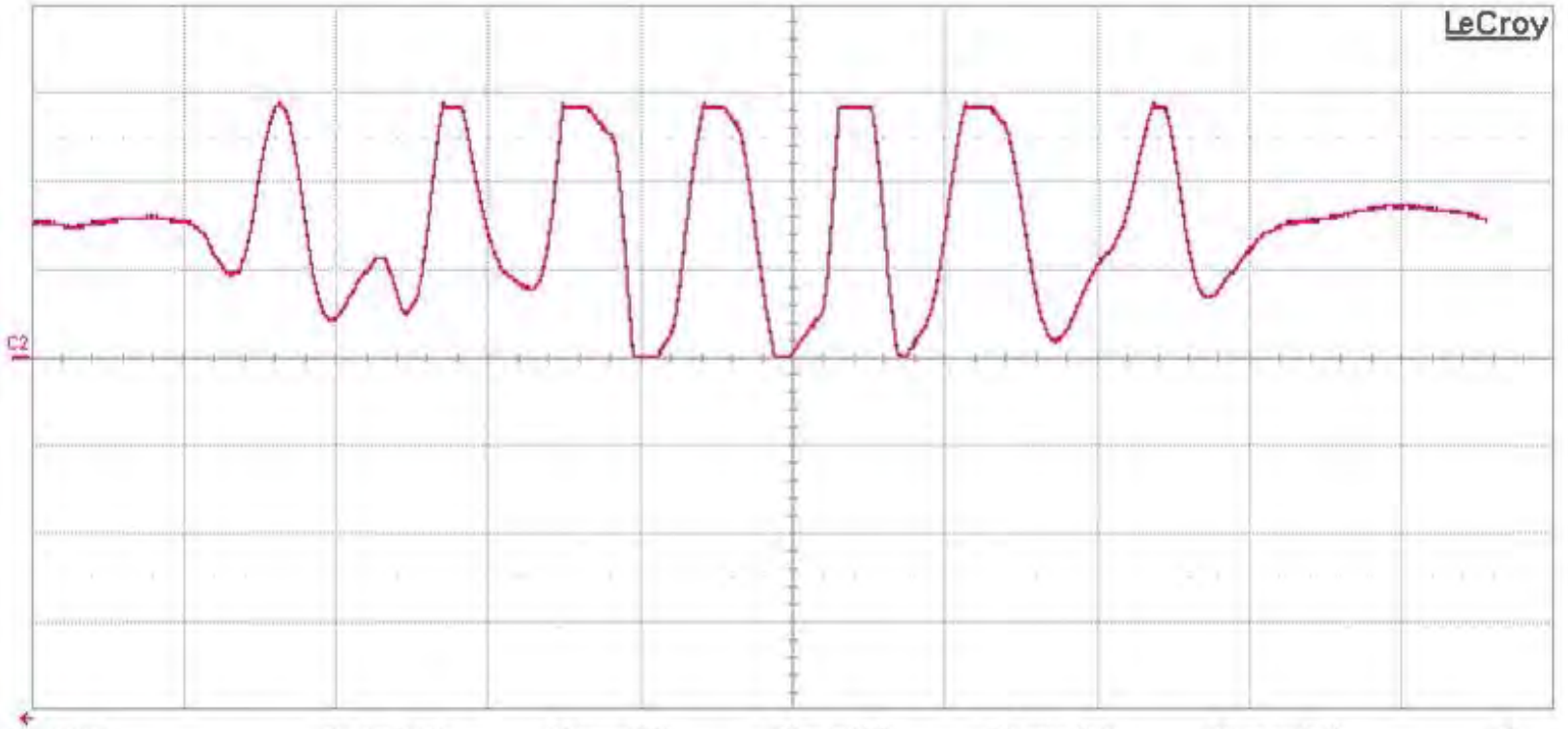


Figure: Virtual Pixel Array

Top View Of The Beams



Intruder Signature For $3m$ Slow Walk



Measure	P1:freq(C2)	P2:max(C2)	P3:min(C2)	P4:rms(C2)	P5:sdev(C2)	P6:- - -
value	864.6472 mHz	2.899 V	4 mV	1.7149 V	816.4 mV	
mean	1.077947746 Hz	2.89939 V	4.25 mV	1.714920 V	816.396 mV	
min	859.8882 mHz	2.899 V	4 mV	1.7149 V	816.4 mV	
max	1.3320151 Hz	2.899 V	4 mV	1.7149 V	816.4 mV	
sdev	176.534431 mHz	---	---	---	---	
num	6	1	1	1	1	
status		✔	✔	✔	✔	

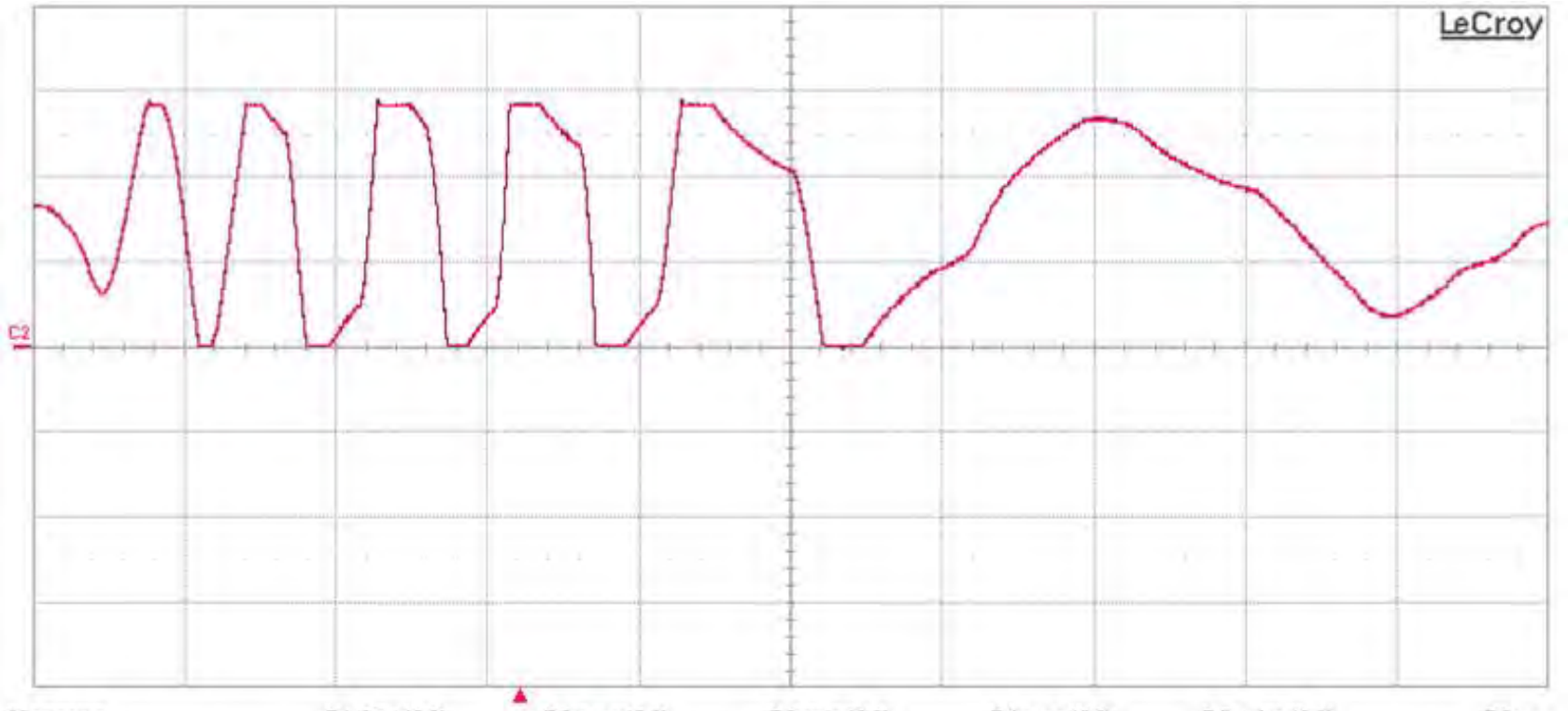
C2 FLT DC 1M
1.00 V/div
0.0 mV ofst

Timebase -13.30 s
Roll 1.00 s/div
250 kS 25 kS/s

Trigger C3 DC
Stop 25 mV
Edge Positive



Intruder Signature For $(50^\circ, 1.5m)$ Slow Walk



Measure	P1:freq(C2)	P2:max(C2)	P3:min(C2)	P4:rms(C2)	P5:sdev(C2)	P6:- - -
value	482.2092 mHz	2.886 V	-2 mV	1.7552 V	951.7 mV	
mean	1.008426152 Hz	2.88576 V	-1.87 mV	1.755241 V	951.696 mV	
min	482.2092 mHz	2.886 V	-2 mV	1.7552 V	951.7 mV	
max	1.4156645 Hz	2.886 V	-2 mV	1.7552 V	951.7 mV	
sdev	307.677150 mHz	---	---	---	---	
num	5	1	1	1	1	
status	✔	✔	✔	✔	✔	

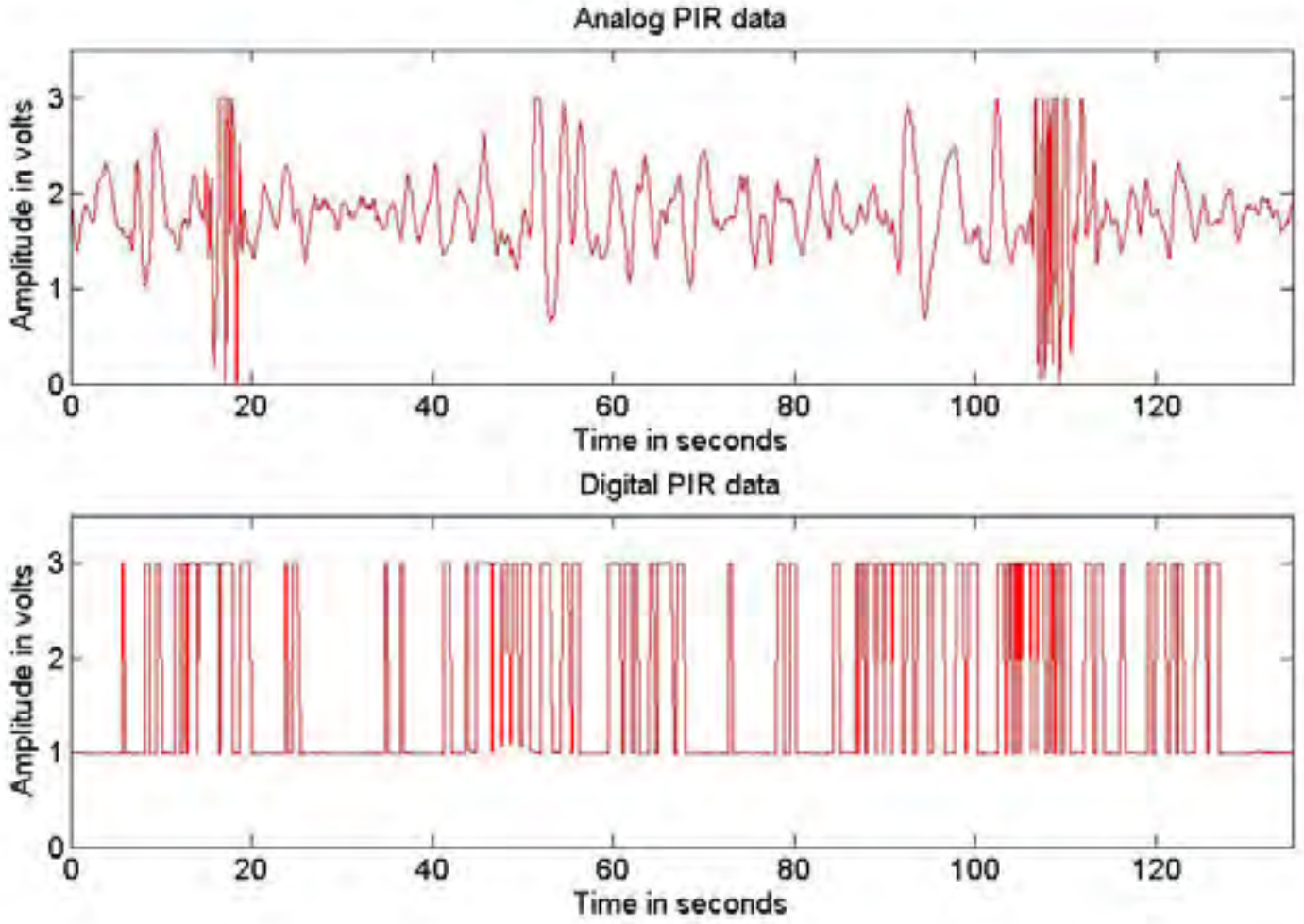
C2 FLT DC1M
1.00 V/div
0.0 mV ofst

Timebase -1.78 s
Roll 1.00 s/div
250 kS 25 kS/s

Trigger C3 DC
Stop 25 mV
Edge Positive



Choice Of Sensor



Transform Based Approach

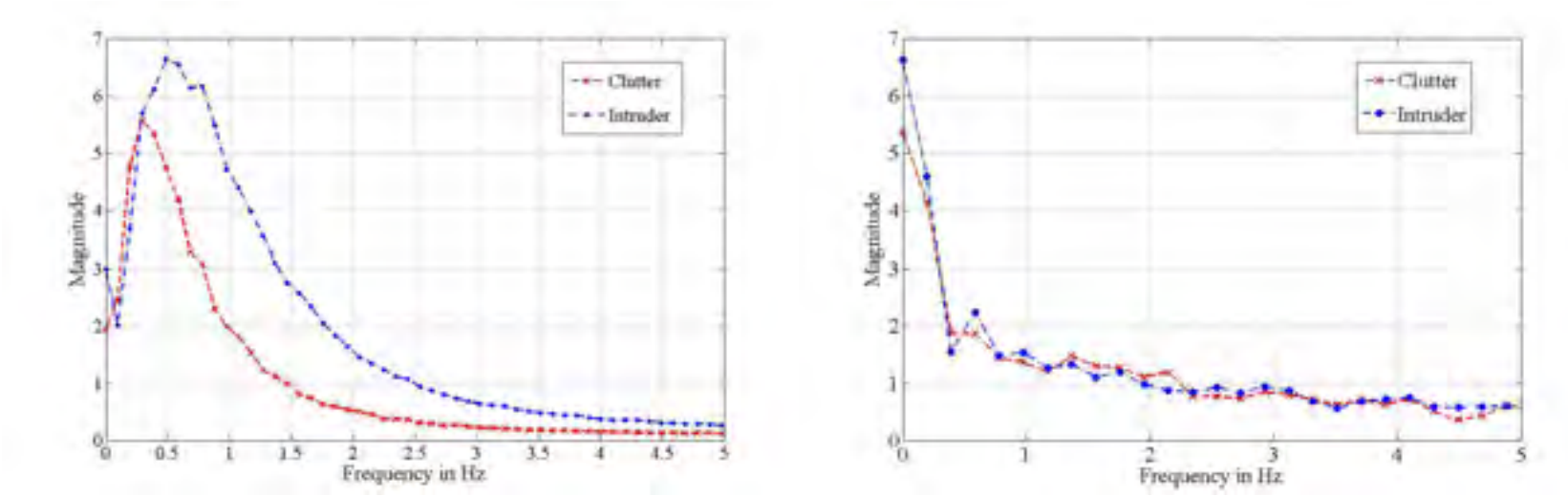


Figure: 256 Pt DFT Of Intruder And Clutter Data From Analog And Digital Sensor.

- The figure above pertaining to the analog sensor suggests separating intruder from clutter based on the spectral signature of their waveforms.
- It was decided to use Haar Transform (HT) for computing the spectral signature in preference to DFT as only additions and subtractions suffice to compute the HT.

The Haar Transform And Frequency Binning

- Since HT is a wavelet transform its coefficients are designed to provide both frequency and time localization information.
- As a result, the breakdown of N Haar coefficients is as follows: there is one coefficient assigned to frequency 0 (the DC component) and 2^k coefficients attached to signals of frequency 2^k, $0 \leq k \leq \log(N) - 1$. Thus, there are a total of $\log(N) + 1$ frequencies or frequency 'bins' for which the energy is computed in the algorithm.
- The Haar signals associated with 8-sample transform are shown in the figure below:

$$\begin{bmatrix} 1 & 1 & 1 & 1 & 1 & 1 & 1 & 1 \\ 1 & 1 & 1 & 1 & -1 & -1 & -1 & -1 \\ 1 & 1 & -1 & -1 & 0 & 0 & 0 & 0 \\ 0 & 0 & 0 & 0 & 1 & 1 & -1 & -1 \\ 1 & -1 & 0 & 0 & 0 & 0 & 0 & 0 \\ 0 & 0 & 1 & -1 & 0 & 0 & 0 & 0 \\ 0 & 0 & 0 & 0 & 1 & -1 & 0 & 0 \\ 0 & 0 & 0 & 0 & 0 & 0 & 1 & -1 \end{bmatrix}$$



The Fast Haar Transform

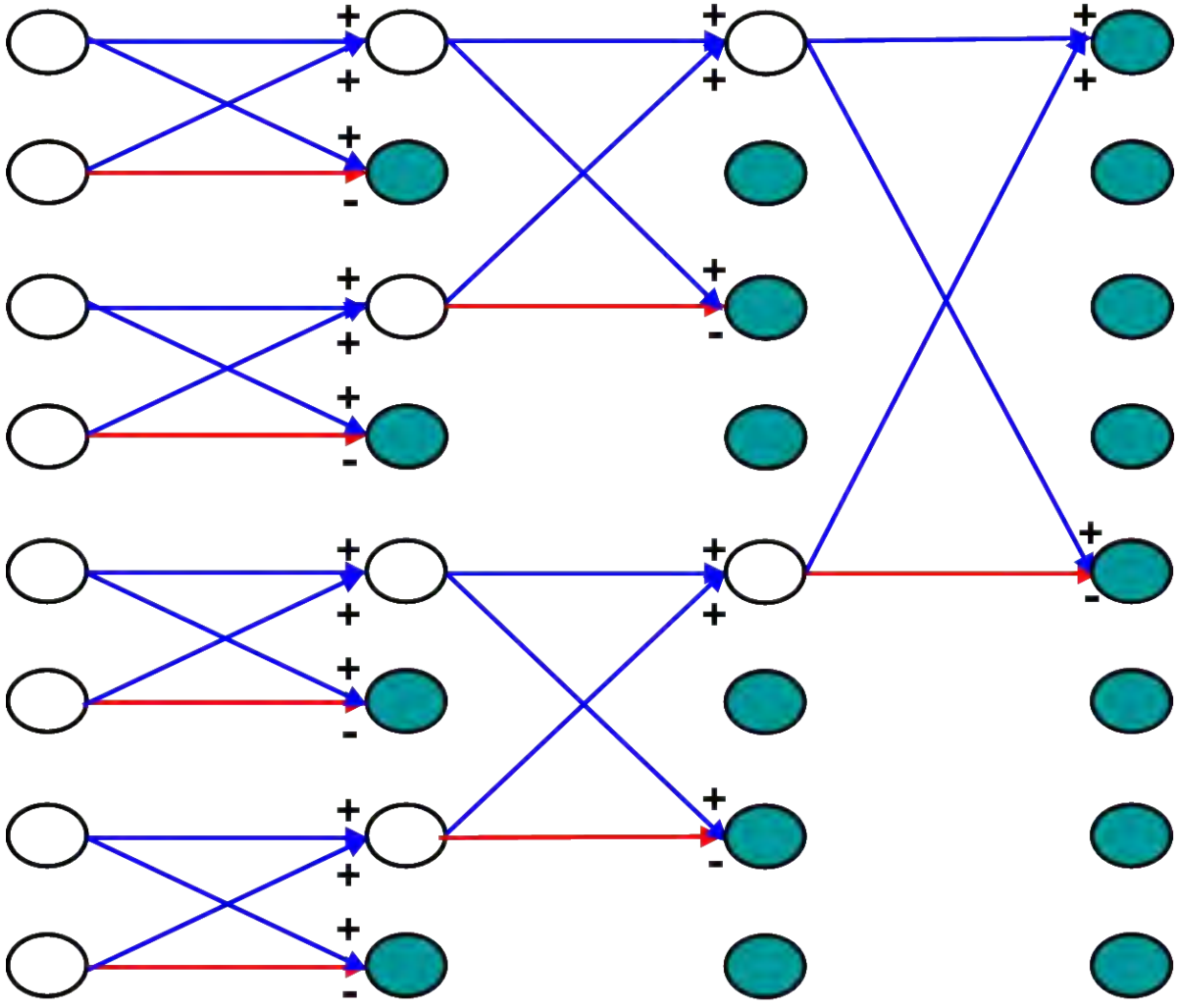
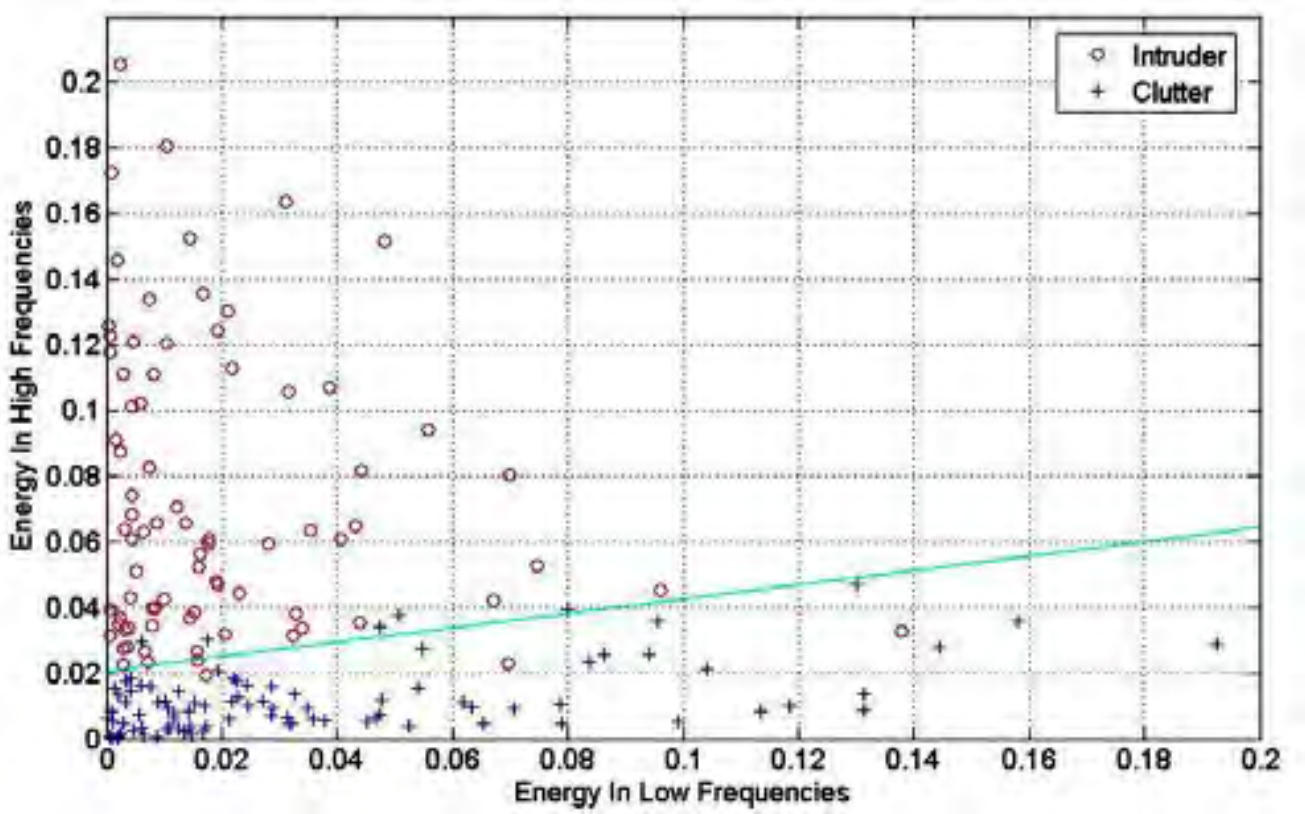


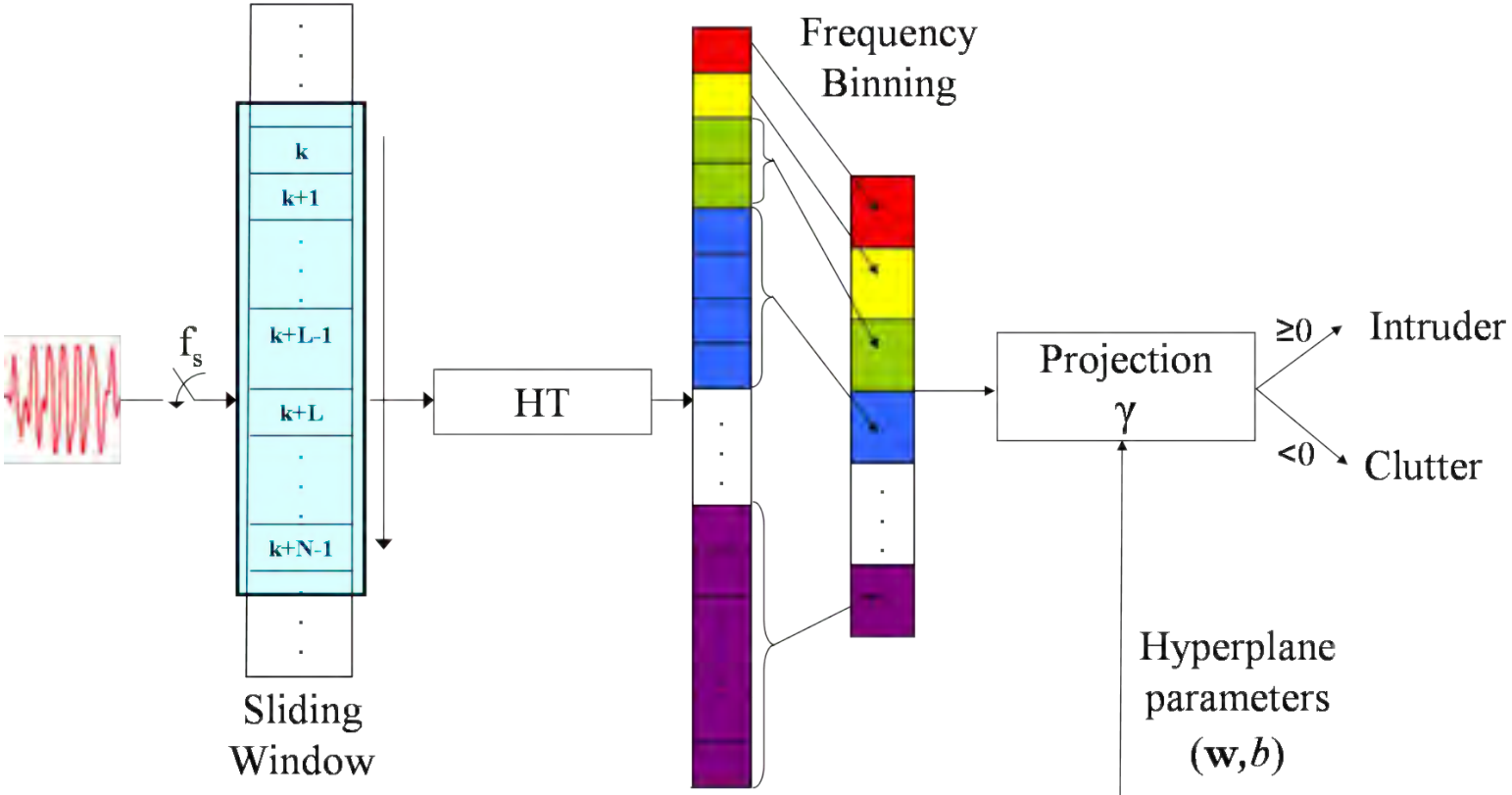
Figure: 8-sample fast Haar transform.

Support Vector Machine



- LIBSVM library interfaced to MATLAB was used for support vector classification.

Functional Block Diagram Of The Algorithm



Computational Complexity

Computations	Additions/ Subtractions	Multiplications	Additions/ Subtractions	Multiplications
FHT	2(N-1)	-	2(N-1)	-
Binning	N-logN	N	N-logN	N
SVM	**Linear SVM**		**Quadratic SVM**	
	1+logN	1+logN	0.5(1+logN)(4+logN)	(1+logN)(3+logN)
Total Computations	3N-1	N+logN+1	3N+0.5(1+logN)(2+logN)-1	N+(1+logN)(3+logN)

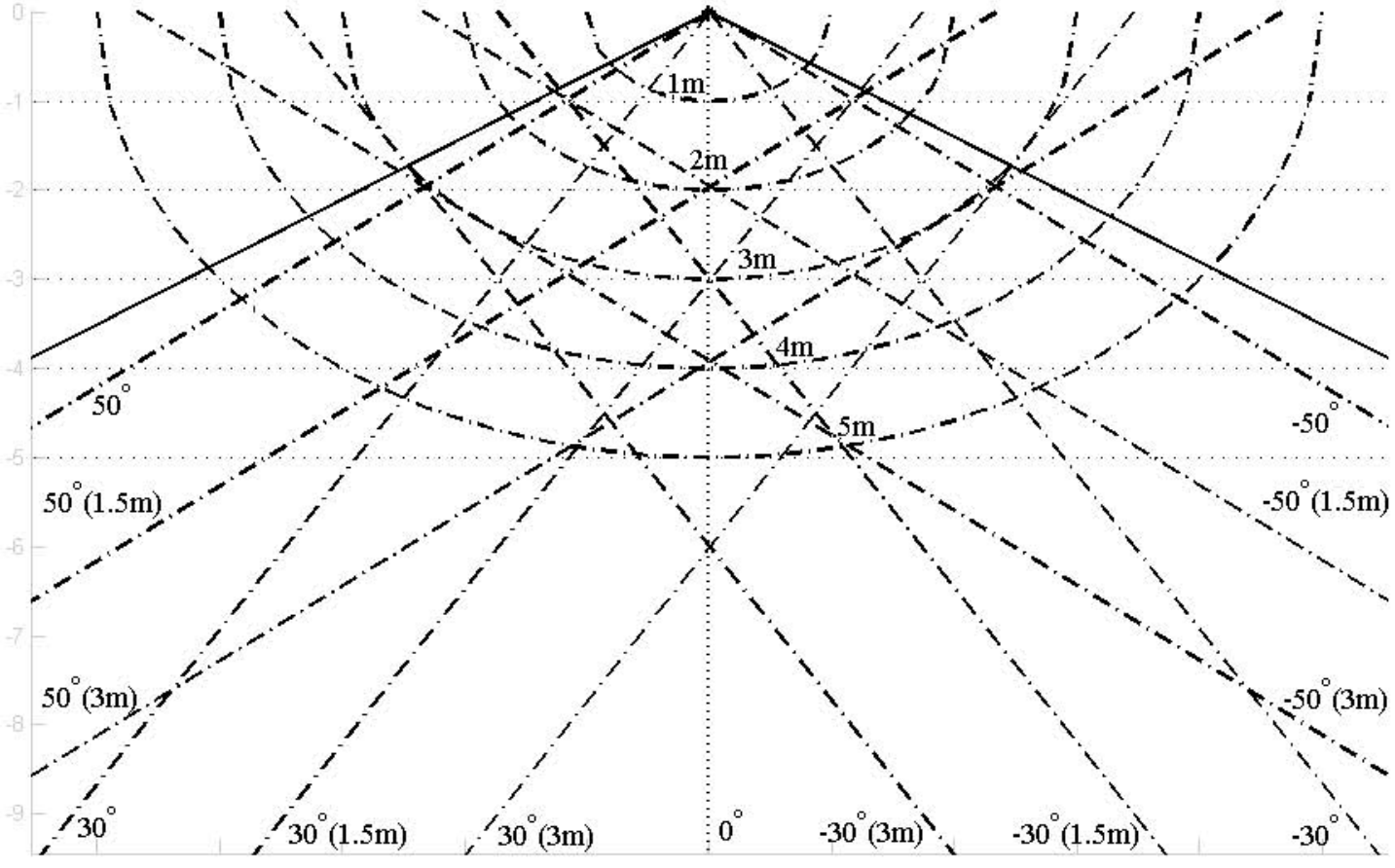
Intruder Data Collection

- Intruder data was collected in a laboratory (i.e., clutter-free) environment.



Figure: Experimental floor layout.

Intruder Data Collection



Clutter Data Collection

- Clutter data was collected across many outdoor locations in IISc over the period October 2008 to March 2009.



Figure: ECE Dept. lawn with a variety of vegetation.

Clutter Data Collection



Figure: A location in ECE Dept. lawn where a part of clutter data was accumulated.

Training Performance

- Performance: (112 Intruder data and 112 Clutter data)
  - $7/112 = 6.3\%$ misses.
  - $4/112 = 3.6\%$ false alarms.



Testing Performance

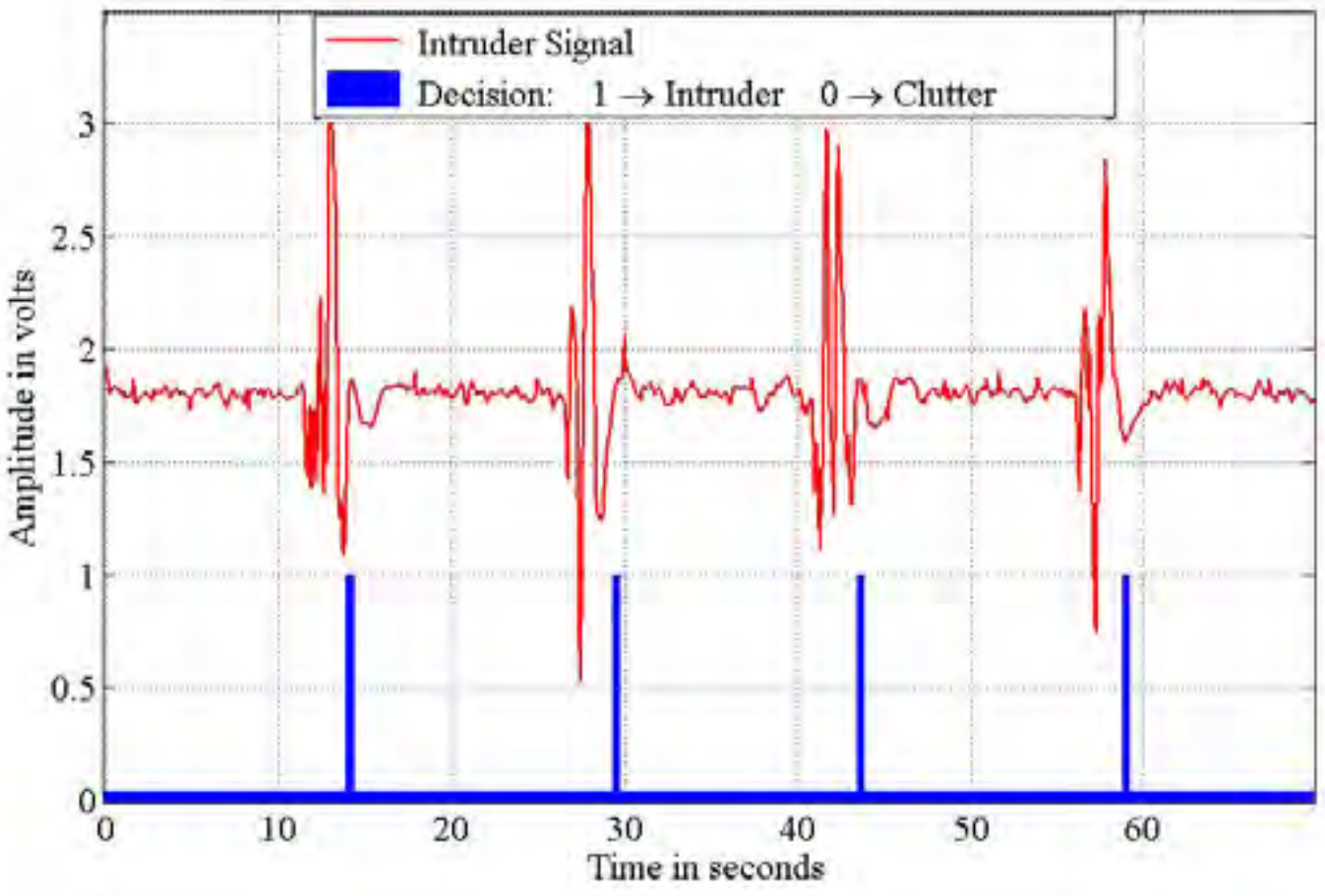


Figure: Linear SVM: Intrusion detected.

Testing Performance

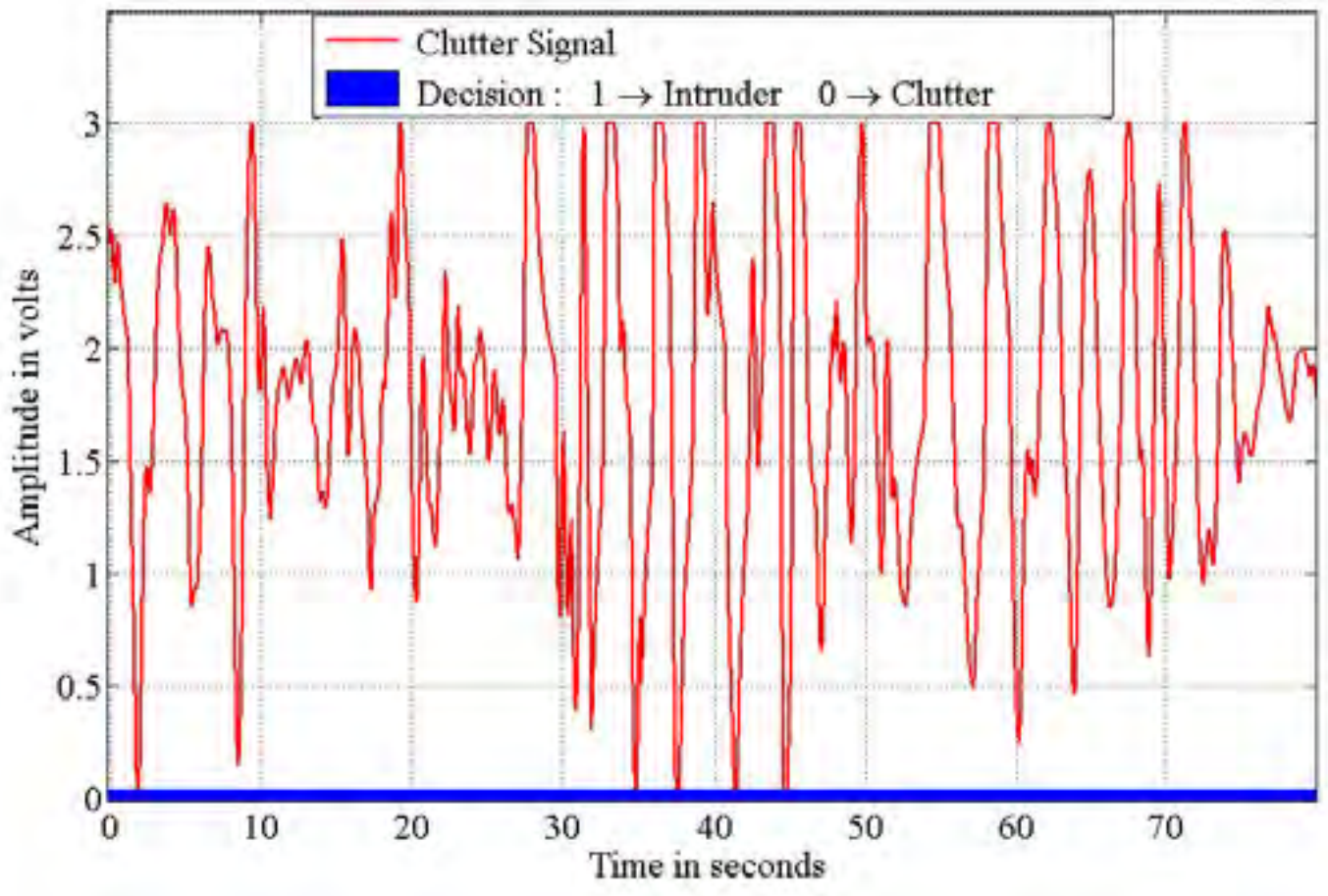


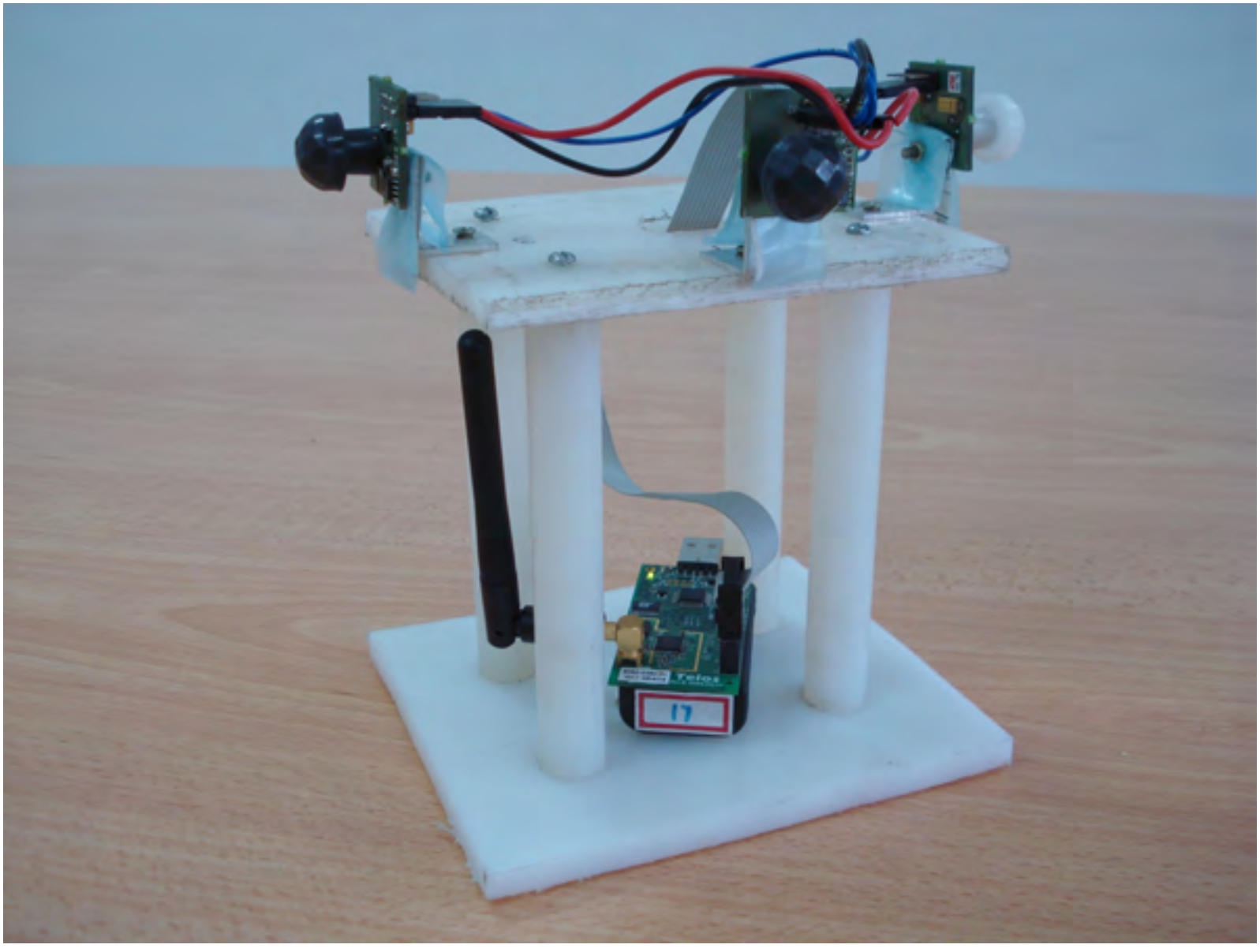
Figure: Linear SVM: Clutter rejected.

Field Testing

- The field testing was conducted in the ECE Dept. lawn.
- Three sensors were mounted onto a single platform each with an angular spacing of 120°. This essentially gave each platform an omni-directional sensing range.
- Two identical, linear and parallel arrays of nodes spaced apart by 5m was laid. The inter-node distance in an array was chosen to maximize the area covered by a single node while ensuring that every point in the sensing range was covered by at least 3 nodes.
- When tested over a period of several hours the network performed flawlessly by detecting every intrusion at speeds ranging from that of a slow crawl to a sprint at 5m/sec. There were also no false alarms in the period over which testing was conducted.



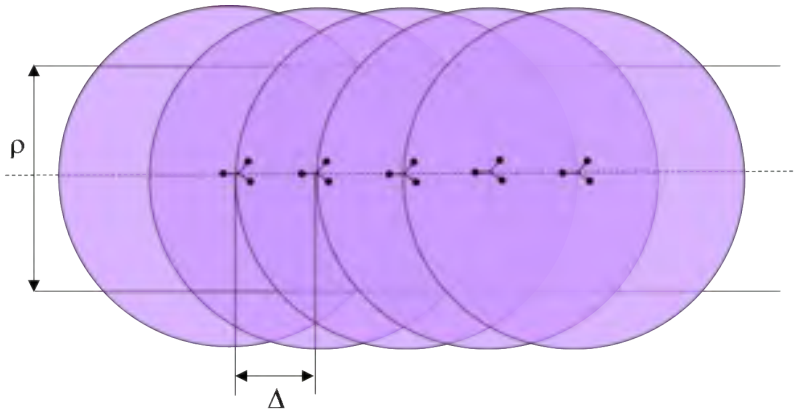
Our Three Sensor Platform



A Field Location



Wireless Trip Wire



- We refer to the linear arrangement of nodes as a 'wireless trip wire'.
- Let Δ, R_s and $(a - p - n)$ be the inter-node distance, sensing radius of a node and area per node respectively.
- Let the trip wire provide us k-coverage for a width of $\frac{\rho}{2}$ on either sides with the $(a - p - n)$ maximized.
- $\Delta = \frac{\sqrt{2}R_s}{k-1}$ maximizes the $(a - p - n)$

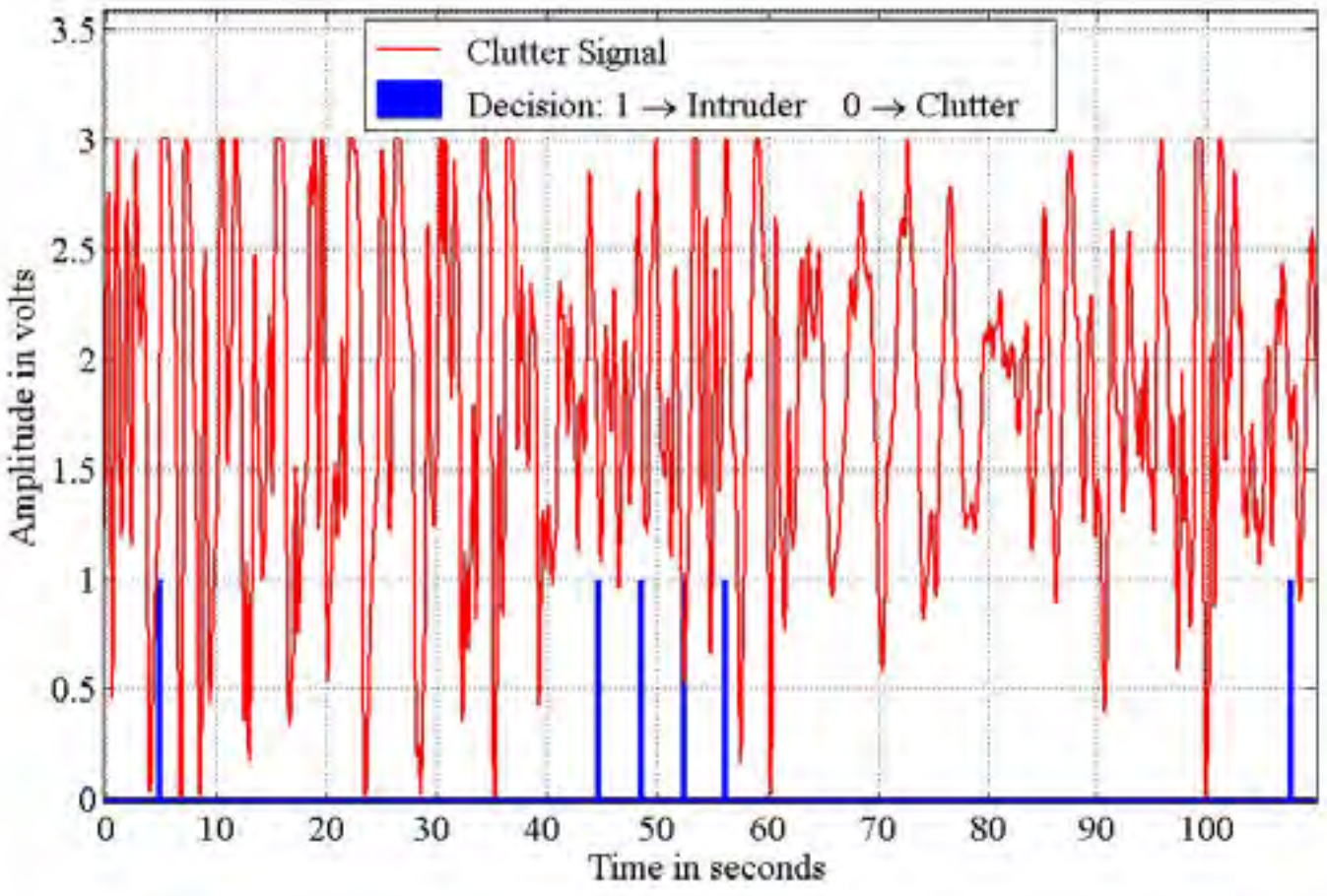
$$(a - p - n)_{max} = \frac{2R_s^2}{k}$$

Limitations

- When field testing was carried out around noontime in April 2009, at the height of the summer in Bangalore, a significantly larger false alarm rate was observed.
- When such summer noontime data was also included in the training set, linear SVM recorded a training performance of $60/275 = 21.8\%$ misses and $22/275 = 8\%$ false alarms.
- Replacing the linear SVM with a quadratic SVM was able to improve the record on training data to $47/275 = 17\%$ misses and $15/275 = 5.5\%$ false alarms.
- The improvement with regard to testing data (simulation) was far more pronounced.



Quadratic SVM On Summer Clutter Data



Summary Of Training Performance

Training Data Set	Linear SVM	Quadratic SVM
Winter Data	95%	-
Winter & Summer Data	85%	88%

Factors Influencing Clutter

- Amplitude of clutter signal depends on
  - Proximity and size of the vegetation.
  - The ambient temperature.
- Frequency depends on
  - Stem's stiffness of the vegetation.
  - The wind speed.



Idealized Intruder Waveform Analysis

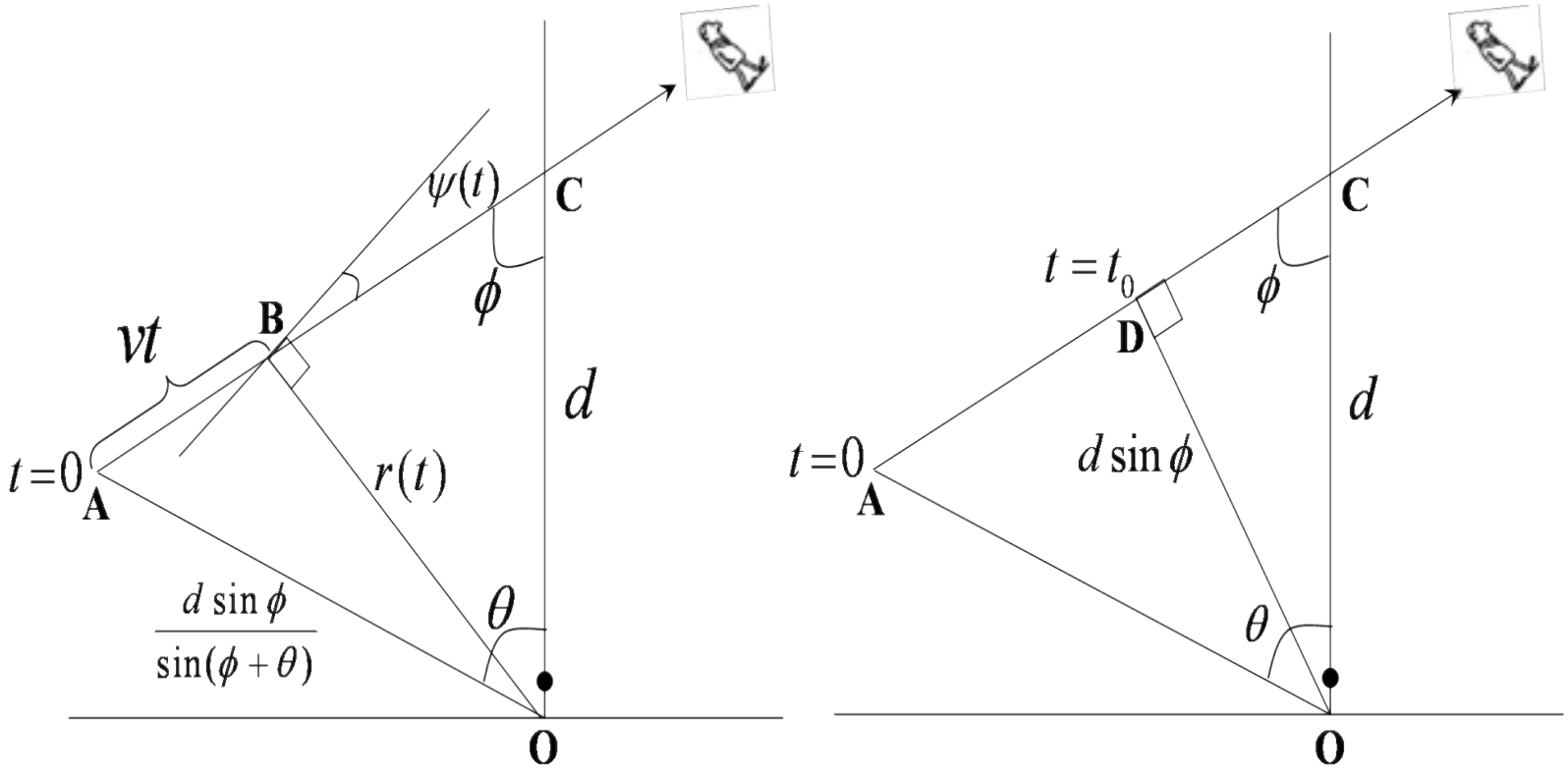


Figure: Geometry used for modeling intruder signature.

Analytical Model For Intruder Signature

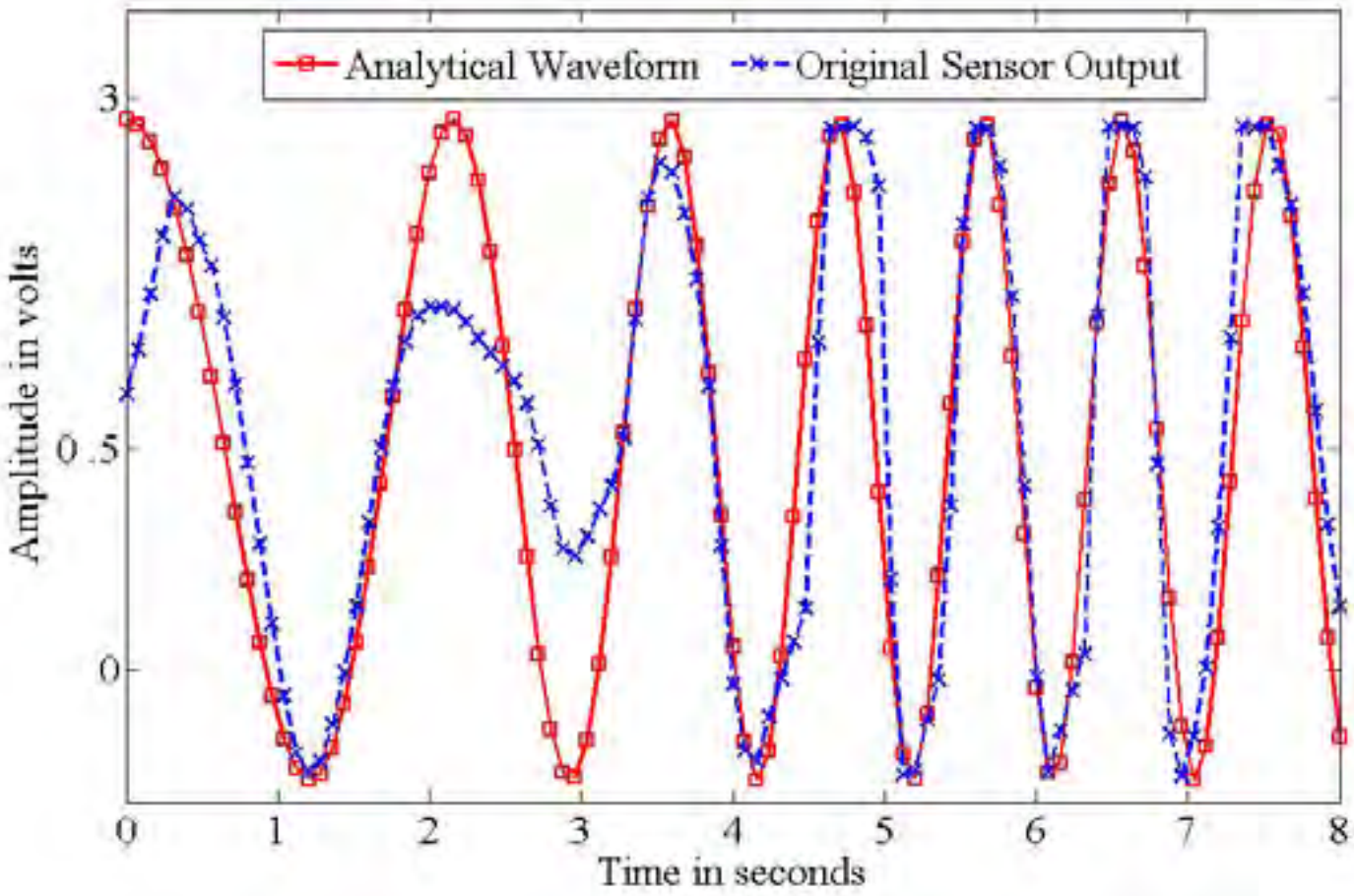
- The instantaneous frequency $f(t)$ of the intruder signature is then from $\triangle OBC$ given by,

$$f(t) = \kappa\omega(t) = \kappa\frac{v\cos\psi(t)}{r(t)} = \frac{\kappa\lambda}{(\lambda(t-t_0))^2+1}$$

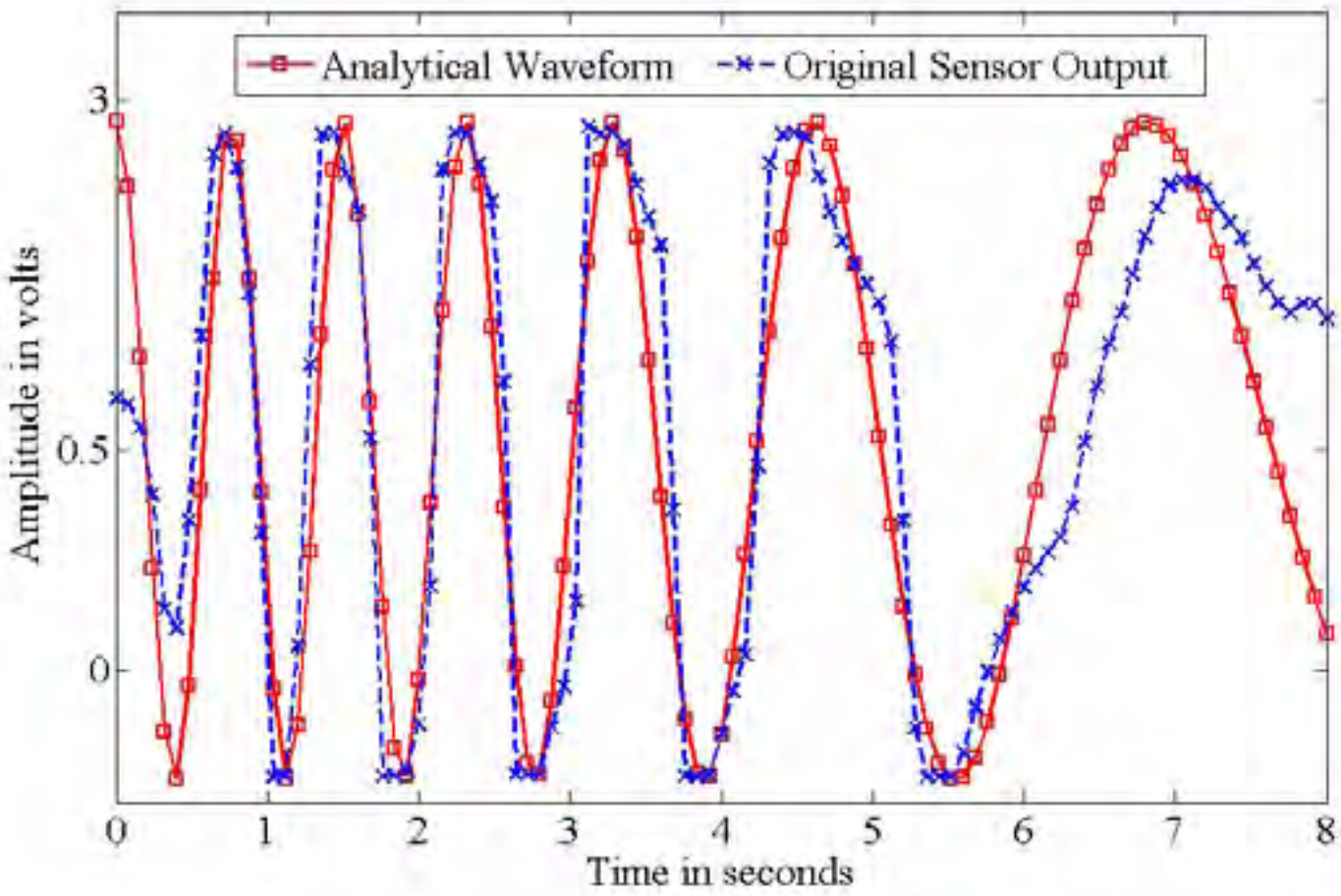
  where $\lambda = \frac{v}{d\sin\phi}$ and $t_0 = \frac{-\cot(\phi+\theta)}{\lambda}$.
- The intruder signature is thus given by,

$$\begin{aligned} s(t) &= \sin\left(2\pi\int_0^t f(t)dt\right) \\ &= \sin\left(2\pi\kappa\arctan\left[\frac{\lambda t}{\lambda^2 t_0(t-t_0)+1}\right]\right) \end{aligned}$$

Intruder Signature For $(v, d, \phi) = (0.7, 3, 90^\circ)$



Intruder Signature For $(v, d, \phi) = (0.3, 2, 50^\circ)$



What Does The Model Suggest?

- κ is the constant which corresponds to the density of the beams.
- Hence the analytical expression naturally extends to other differential PIR sensors in general as κ abstracts the lens.
- λ and t_0 determine the intruder's analytical waveform.
- λ for different triplets of (v, d, ϕ) can be the same. Hence velocity and direction of motion information from a single sensor cannot be extracted.
- λ corresponding to colocated sensors will be identical. Hence velocity and direction of motion information also cannot be obtained from multiple sensors on the same node.
- So to track the intruder, many sensing nodes spaced apart will be required.



Tracking

- Let the coordinates of the sensing nodes be (x_i, y_i).
- Set $\eta_i = 1/\lambda_i$.
- Lets assume that the ith sensor node has available its reliable estimate of η_i.
- Let the intruder path equation be $ax + by + c = 0$.
- Set $r = \frac{\sqrt{a^2+b^2}}{c}$ and $\alpha = \arctan\left(\frac{a}{b}\right)$.
- The intruder path equation $ax + by + c = 0$ can be rewritten as: $xr \sin\alpha + yr \cos\alpha + 1 = 0$.

Tracking

- For a node at (x_1, y_1),

$$\begin{aligned} d_{min,1} &= \frac{ax_1 + by_1 + c}{\sqrt{a^2 + b^2}} \\ \Rightarrow \eta_1 &= \frac{d_{min,1}}{v} = \frac{\sin\alpha}{v}x_1 + \frac{\cos\alpha}{v}y_1 + \frac{1}{vr} \end{aligned}$$

- We have 3 unknowns, r, α, v but just one equation. Thus we require two more equations to solve for r, α and v.

$$\begin{aligned} \eta_2 &= \frac{\sin\alpha}{v}x_2 + \frac{\cos\alpha}{v}y_2 + \frac{1}{vr} \\ \eta_3 &= \frac{\sin\alpha}{v}x_3 + \frac{\cos\alpha}{v}y_3 + \frac{1}{vr} \end{aligned}$$

Now we have 3 equations in 3 unknowns.



Tracking

- After some work, it can be shown that

$$
\begin{aligned}
v &= \frac{1}{\sqrt{s^2 + c^2}} \\
\alpha &= \arctan\left(\frac{s}{c}\right) \\
r &= \frac{1}{v\left(\eta_3 - sx_3 - cy_3\right)}
\end{aligned}
$$

where

$$
\begin{aligned}
s &= \frac{\sin\alpha}{v} = \frac{(\eta_1 - \eta_2)(y_1 - y_3) - (\eta_1 - \eta_3)(y_1 - y_2)}{(x_1 - x_2)(y_1 - y_3) - (x_1 - x_3)(y_1 - y_2)} \\
c &= \frac{\cos\alpha}{v} = \frac{-(\eta_1 - \eta_2)(x_1 - x_3) + (\eta_1 - \eta_3)(x_1 - x_2)}{(x_1 - x_2)(y_1 - y_3) - (x_1 - x_3)(y_1 - y_2)}
\end{aligned}
$$

- Hence, **3 sensing nodes** will suffice in reliably tracking the intruder.



Optimal Locationing Of The 3 Sensing Nodes

- Tracking involves the transformation: $(\eta_1, \eta_2, \eta_3) \rightarrow (r, \alpha, v)$.
- The impact of error in the estimates of η_i's on r, α and v should be kept minimum for reliable tracking.
- Equivalently, the Jacobian of the transformation carrying out the mapping: $(r, \alpha, v) \rightarrow (\eta_1, \eta_2, \eta_3)$ should be maximized.

$$J \doteq \begin{vmatrix} \frac{\partial \eta_1}{\partial r} & \frac{\partial \eta_2}{\partial r} & \frac{\partial \eta_3}{\partial r} \\ \frac{\partial \eta_1}{\partial \alpha} & \frac{\partial \eta_2}{\partial \alpha} & \frac{\partial \eta_3}{\partial \alpha} \\ \frac{\partial \eta_1}{\partial v} & \frac{\partial \eta_2}{\partial v} & \frac{\partial \eta_3}{\partial v} \end{vmatrix}$$

- Without loss of generality lets assume a coordinate system whose origin is equidistant from the three sensors. Each sensor then is at a constant distance R from the origin.

Optimal Locationing Of The 3 Sensing Nodes

- Again we have a system of 3 equations in the 3 unknowns r, α and v:

$$\eta_i = \frac{\sin\alpha}{v} x_i + \frac{\cos\alpha}{v} y_i + \frac{1}{vr}, \quad 1 \leq i \leq 3.$$

- Rewriting the above system of 3 equations with $x_i = R\cos(\beta_i)$, $y_i = R\sin(\beta_i)$, where $\beta_i = \arctan(\frac{y_i}{x_i})$, we have

$$\eta_i = \frac{R}{v}\sin(\alpha + \beta_i) + \frac{1}{vr}, \quad 1 \leq i \leq 3.$$

- After some work, it can be shown that this Jacobian is given by

$$J = \frac{R^2}{r^2 v^2}\left[\sin(\beta_3 - \beta_2) + \sin(\beta_1 - \beta_3) + \sin(\beta_2 - \beta_1)\right].$$



Optimal Locationing Of The 3 Sensing Nodes

- The value of J is clearly maximized when $\beta_3 - \beta_2 = \beta_1 - \beta_3 = \beta_2 - \beta_1 = \frac{2\pi}{3}$ and when R is made as large as possible.
- This suggests that the **nodes should be arranged in an equilateral triangle** with R as large as possible, subject to the desired node density.



Other Issues

- With a good model for the clutter signature, this problem can be formulated into a proper detection problem.
- Sleep-wake cycling.
- Online training.



Conclusion

- We have reasonably met the challenges.
- This application will become sophisticated when ‘better’ sensors become available.



References

- S. Oh, P. Chen, M. Manzo, and S. Sastry, "Instrumenting wireless sensor networks for real-time surveillance," in *Proc. of the International Conference on Robotics and Automation*, May 2006.
- A. Arora, P. Dutta, S. Bapat, V. Kulathumani, H. Zhang, V. Naik, V. Mittal, H. Cao, M. Demirbas, M. Gouda, Y-R. Choi, T. Herman, S. S. Kulkarni, U. Arumugam, M. Nesterenko, A. Vora, and M. Miyashita, "A line in the sand: A wireless sensor network for target detection, classification, and tracking", Ohio State University, 2003.
- MP Motion Sensor (AMN 1,2,4) data sheet, Panasonic Electric Works Corporation of America, New Jersey, USA.
- Sidney B. Lang, "Pyroelectricity: From Ancient Curiosity to Modern Imaging Tool", *Physics Today*, pages 31-36, Aug. 2005.



Questions




THANK
YOU